

Natural Gas Hydrate Particles in Oil-Free Systems with Kinetic Inhibition and Slurry Viscosity Reduction

Minwei Sun[†] and Abbas Firoozabadi^{*,†,‡}

[†]Reservoir Engineering Research Institute, 595 Lytton Avenue, Suite B, Palo Alto, California 94301, United States

[‡]Yale University, 9 Hillhouse Avenue, New Haven, Connecticut 06511, United States

ABSTRACT: Petroleum fluids may form hydrate crystals with water at conditions often encountered in nature. Hydrate formation in large pieces is a serious problem in flow assurance and oil capture from the seabed. Use of functionalized molecules in very small quantities offers effective solution through formation of small hydrate particles. The literature suggests water-in-oil emulsion for hydrate antiagglomeration, which limits the application because of requirement of large amounts of the oil phase. In a recent article, we have demonstrated hydrate antiagglomeration of methane in water and brine by a new surfactant molecule at 0.2 wt % without water-in-oil emulsion. However, in a natural gas containing CO₂, the same surfactant loses effectiveness. In this work we offer a revised formulation consisting of the surfactant, small amounts of a base, and an alkane. The base adjusts the pH, and the alkane serves as a defoamer. The effects of each component are systematically discussed in this work, and a synergistic effect is found. The new formulation provides effective antiagglomeration in a broad range of conditions. Moreover, our formulation has three other beneficial effects including kinetic inhibition, reduction of slurry viscosity, and corrosion inhibition.

■ INTRODUCTION

Water often forms gas hydrates with small gas molecules (e.g., methane, ethane, propane, carbon dioxide, nitrogen) in oil and natural gas flowlines at temperatures as high as 20 °C and pressures as low as 50 bar.^{1–3} Risk management of gas hydrates is a major challenge in offshore hydrocarbon production. Formation of hydrate particles rather than a large piece of hydrates is perhaps the best solution in deep water where the subcooling is high and alternatives such as kinetic inhibition are not effective.^{2,4,5} This approach is referred to as hydrate antiagglomeration (AA) in the natural gas hydrate literature. The main limitation to application has been the need for large quantities of oil because of the type of surfactants that have been used and the perceived mechanisms.^{2,6–12} Little progress has been made in antiagglomeration at high watercuts, which are often the case in natural gas flowlines.

Prior to publication of our recent work (Sun and Firoozabadi, 2013),⁵ the general belief in the hydrate literature has been that an oil phase in large quantities is required for hydrate antiagglomeration.^{13–17} The mixtures of oil/water/surfactant have been required to form water-in-oil emulsion from which hydrate particles can be dispersed in the oil phase when the conditions fall into the hydrate regime.^{2,13} We have demonstrated that hydrate antiagglomeration can be realized in water-in-oil emulsions, in oil-in-water emulsions, and also from micelles in which there is no oil phase.⁵ We have performed extensive set of experiments using a new surfactant in methane hydrates demonstrating hydrate slurries in oil/water and in water (or brine) systems. The tests have revealed the superiority of the new surfactant in methane hydrates over quaternary ammonium salts. Our work was the first report of antiagglomeration of methane hydrates without the oil phase.

In this paper, we expand hydrate antiagglomeration from methane hydrates to natural gas hydrates. Methane often forms structure I (sI) hydrates, and natural gas often forms structure

II (sII) hydrates. Natural gas is a mixture of methane and various quantities of other alkanes (e.g., ethane, propane, etc.), alkenes, and aromatics, carbon dioxide, nitrogen, and hydrogen sulfide.¹³ Acid gases, such as CO₂ and H₂S, decrease the pH in the aqueous phase. Corrosion of carbon steel by CO₂ and H₂S at low pH is a major problem in the oil and gas industry.^{18,19} In this study, we discover that CO₂ in the natural gas affects hydrate antiagglomeration with the new surfactant. There are vast differences between antiagglomeration of methane and natural gases with respect to the surfactant we have used successfully in methane hydrates. A new AA formulation is developed to address the challenges from acid gases in natural gas. Our revised formulation has other desirable effects, including kinetic inhibition and viscosity reduction of hydrate slurry. The effective component in methane hydrate antiagglomeration is cocamidopropyl dimethylamine surfactant. Our new formulation consists of the same surfactant, a pH adjuster (sodium hydroxide or potassium hydroxide), and a small amount of oil (*n*-octane). The new formulation is highly effective in hydrate antiagglomeration of natural gas at 100% watercut in both freshwater and 1.5 wt % NaCl brine.

■ MATERIALS AND METHODS

The same experimental setup as in ref 5 is used in this work. The experiments are performed in a sapphire rocking cell apparatus (by PSL Systemtechnik) shown in Figure 1. Each cell has a volume of 20 mL equipped with a stainless steel ball to aid agitation. In each test, the cells are charged with 10 mL liquid samples. The water bath is filled before the cells are pressurized with a test gas to the desired pressure. The rocking frequency is set to 15 times/min. The bath temperature, the pressure, and ball running time during rocking (the time the ball travels between the two position sensors that are apart by 80 mm; see

Received: December 20, 2013

Revised: February 14, 2014

Published: February 21, 2014

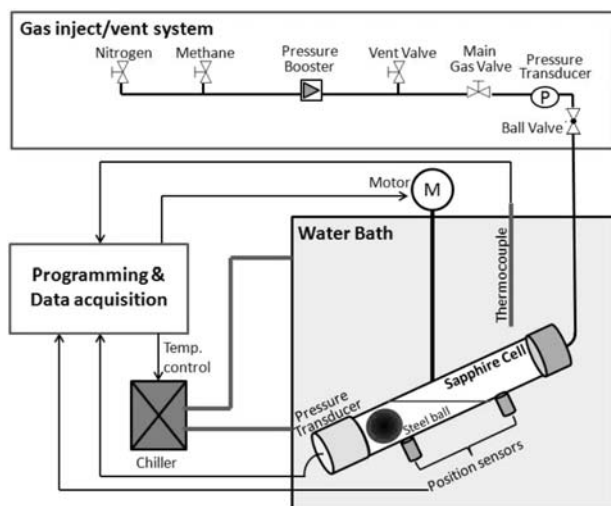


Figure 1. Gas hydrate sapphire rocking cell setup.

Figure 1) are recorded. Figure 1 shows a schematic of the setup. At the start after charging the cells with various fluids, they are rocked at 20 °C (24 or 28 °C) for half an hour to reach equilibrium, which is set as the initial condition of the closed cell test. Then the water bath is cooled from room temperature to 2 °C at different cooling rates varying from -2 to -10 °C/h while the cells are being rocked. The cells are then kept at 2 °C for a period of time, allowing the gas hydrates to fully develop before the temperature ramps back to the initial temperature. Sharp pressure changes indicate hydrate formation/dissociation. A long ball running time implies high viscosity of the slurry in the cell. The steel ball stops running when hydrate plugging occurs. The effectiveness is evaluated by visual observations and by ball running time. All rocking cell tests are repeated at least two times.

A tensiometer (K12 by Kruss) is used to measure the interfacial tension at 20 °C. Each measurement is repeated 5 times. Dynamic light scattering (ZetaPALS by Brookhaven Instrument Corp.) is used to measure the size of the micelles, emulsions/aggregates in the liquid state at room temperature. All measurements are repeated 10 times.

The AA (from Lubrizol Corporation) contains 80–89% cocamidopropyl dimethylamine (as the effective component, shown in Figure 2), 5–10% glycerin, small amount of free amine, and water. Glycerin

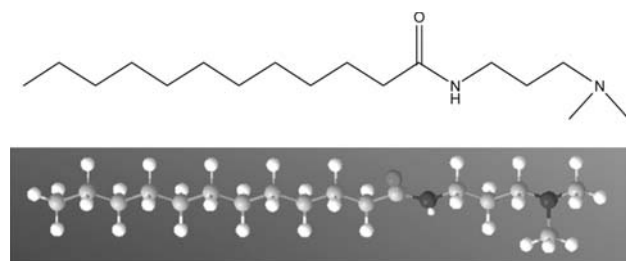


Figure 2. Chemical structures (2D (top) and 3D (bottom)) of the main component in our antiagglomerant. Blue, red, gray, and white spheres represent nitrogen, oxygen, carbon, and hydrogen atoms.

and small amounts of amine and water are byproducts of surfactant synthesis. Since the concentration of these byproducts is very low (<0.05 wt % in the aqueous phase), their thermodynamic effect is expected to be negligible. Sodium hydroxide (NaOH) and potassium hydroxide (KOH) are 99+% pure from Sigma Aldrich, and *n*-octane is from Acros. The composition of the natural gas used in this work is shown in Table 1.

Table 1. Composition of Natural Gas (Mol Basis)

Component, %						
methane	ethane	propane	butane	isobutane	nitrogen	carbon dioxide
80.67	10.20	4.90	0.753	1.53	0.103	1.83

RESULTS AND DISCUSSION

We first use the AA at a concentration of 0.2 wt % in the natural gas at 100% watercut (no oil phase). At this concentration we have observed antiagglomeration in methane hydrates as reported in ref 5. Serious foaming at room temperature in the rocking the cell is observed as shown in Figure 3; there was

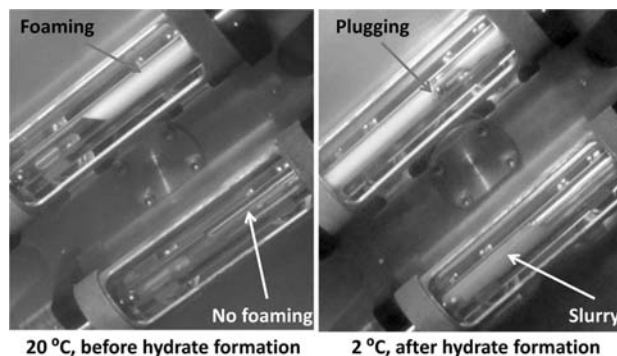
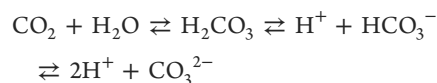


Figure 3. Natural gas: images of rocking cell test before and after hydrate formation. The initial pressure is 87 bar at 20 °C. The cooling rate is -4 °C/h. Top cell contains 10 mL of 0.2 wt % AA solution. Bottom cell contains 10 mL of 0.2 wt % AA + 0.4 wt % NaOH solution.

no foam formation in methane hydrates. The formation of foam increases the gas/liquid interfacial area and reduces the concentration of the surfactant in the aqueous phase. An instant plugging with hydrate formation in the natural gas system is then observed. The top cells in Figure 3 show the images from the foam and the plugged system. The pH of the aqueous/AA mixture before contact with natural gas and after hydrate formation in the rocking cell is measured: fresh 0.2 wt % AA solution has a pH of 10.4; after the test the pH decreases to 6.8. The large pH decrease is due to the following reactions.



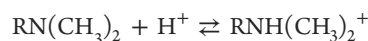
In the methane system there is no change in pH before and after contact of the aqueous phase with methane. We introduced a small amount of NaOH into the solution to adjust the pH. The bottom cells in Figure 3 show the image of the test cells after the introduction of NaOH. There is no formation of foam in the cell. Hydrate particles do not agglomerate, and hydrate slurry can be readily observed. The pH before and after the tests is 12.6 and 10.1, respectively. KOH at the same molar concentration has the same effect as NaOH. We have found that the pH should be maintained above 9 in order to optimize our AA performance, as shown in Table 2 at different test conditions. When the pH is below 9, foam formation and agglomeration are observed. Obviously, NaOH itself does not have antiagglomeration effect.

Table 2. pH before and after Natural Gas Hydrate Test and AA Effectiveness

NaOH, wt %	AA, wt %	<i>n</i> -octane, vol %	initial <i>P</i> (bar) and <i>T</i> (°C)	pH (before)	pH (after)	effectiveness
0.4	0	0	60, 20	12.9	10.4	no
0	0.2	0	37, 20	10.6	7.1	no
0.4	0.2	0	60, 20	12.6	10.1	yes ^a
0.4	0.2	0.2	60, 20	12.6	10.0	yes ^b
0.4	0.2	0	80, 24	12.6	9.3	yes ^a
0.4	0.2	0.2	80, 24	12.6	9.3	yes ^b
0.4	0.3	0.4	100, 28	12.7	8.9	no
0.6	0.3	0.4	100, 28	13.0	9.7	yes ^b
0.6	0.6	0.4	100, 28	13.1	9.9	yes ^b

^aCooling rate = -2 °C/h. ^bCooling rate = -10 °C/h.

Low pH does not only cause foaming but also changes the surfactant interaction with hydrates. Our surfactant molecule, a nonionic amine, reacts with H⁺ as follows,



which affects the AA performance. There is an increase in solubility of the surfactant in water when the pH is low. The above reaction increases the surface tension of 0.2 wt % AA solution from 27.6 mN/m (pH 10.4) to 32.5 mN/m (pH 6.8) at room temperature, which indicates that the concentration of the surfactant has decreased on the surface. In the absence of hydrogen ions in water, the nitrogen atom in the surfactant is the binding site onto hydrate surface by forming N...H hydrogen bond with hydrogen atoms of the hydrate.⁵ At low pH, when there are hydrogen ions in water, the nitrogen atoms of the surfactant bound to them; there are no adequate surfactant molecules left for hydrate antiagglomeration. Therefore, our AA is not effective at low pH. Foaming also takes the surfactant molecules out of the solution.

Another benefit of adding NaOH is the reduction of hydrate slurry viscosity. In Figure 4 we present profiles of pressure, temperature, and the ball running time of hydrate formation in methane and natural gas system. The concentration of the AA is 0.2 wt % for both methane and natural gas tests. In the natural gas test the concentration of NaOH is 0.4 wt %. The blue curves represent the results of methane hydrate test with 0.2 wt % AA. The red curves represent the results of natural gas hydrate test with 0.2 wt % AA and 0.4 wt % NaOH. In both tests we observe hydrate antiagglomeration. In the top figure, the sudden pressure drop in the left indicates hydrate formation. The crystallization temperatures (that is, hydrate formation temperatures) in Figure 4 may be lower than the hydrate equilibrium temperatures. The hydrate equilibrium temperature for methane at 86 bar is 11 °C,¹³ and the hydrate equilibrium temperature for the natural gas at 81 bar is 18 °C.¹² In Figure 4 we observe the formation of hydrates in natural gas at a temperature of 13.1 °C when the pressure has reached 81 bar; therefore, the hydrate formation depression is 4.9 °C. Methane hydrates form at 9.3 °C when the pressure is 86 bar; therefore, the depression is less than 2 °C, which is the same as the test without an additive.⁵ The gas consumption in natural gas is slower than methane, indicating a slower hydrate formation rate. Such findings demonstrate that our new formulation has kinetic inhibiting effect in natural gas hydrates. Methane and natural gas have about the same pressure drops, from 91 to 34 bar for methane and from 87 to 37 bar for

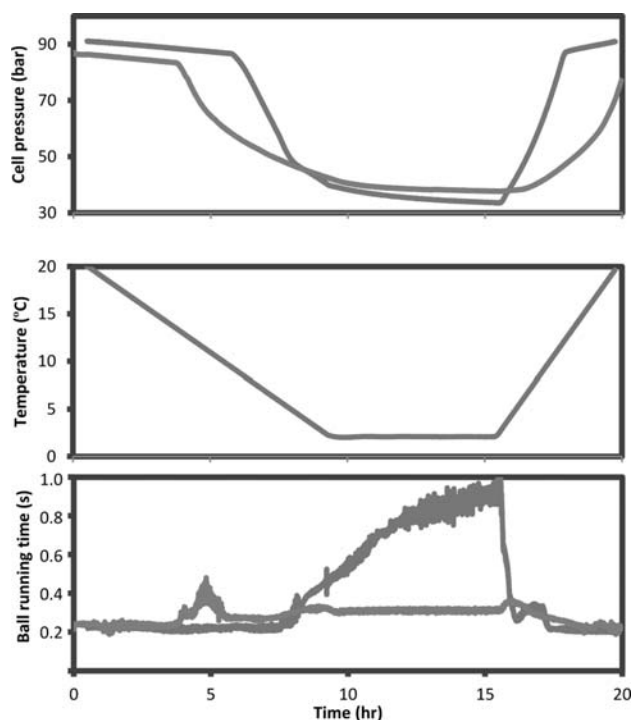
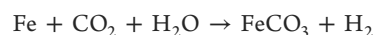


Figure 4. Natural gas and methane: hydrate formation from the initial pressure of 91 bar in methane (blue) and initial pressure of 87 bar in natural gas (red) tests and the initial temperature of 20 °C. The temperature decreases from 20 to 2 °C at a rate of -2 °C/h, then kept at 2 °C for 6 h before ramping back to 20 °C. The watercut is 100%. The concentration of AA is 0.2 wt % in water. In the natural gas test (red), the NaOH concentration is 0.4 wt %.

natural gas, which implies about the same amount of hydrates is formed in these two tests. The ball running time in methane hydrate test ramps up to 1 s when hydrate content increases. However, the ball running time in natural gas hydrate test remains low (below 0.4 s), indicating a low slurry viscosity. Low viscosity allows slurry to flow easily in pipelines.

The low slurry viscosity at about the same hydrate fraction can be explained through the effective hydrate fraction concept.²⁰ When the gas hydrates form in pipeline, the crystalline particles can stick together and turn into large aggregates with a fractal structure that can trap aqueous phase and liquid hydrocarbon in the internal pores. The effective hydrate fraction can be much larger than the true fraction, which is directly correlated to the slurry viscosity. By addition of NaOH, the adsorption of AA molecules on hydrate surface gets enhanced, thus leading to a lower effective hydrate fraction. We have measured hydrate particle size and have noticed that the effective slurry reduction is due to reduction in the size of the hydrate particles. The hydrate particle size data will be published later.

There is also another benefit to the addition of NaOH in our formulation from the increase in the pH in relation to protection of steel pipelines. The pH has a strong influence on the corrosion rate.^{21,22} pH in CO₂-saturated water in pipelines can be below 4, which is highly corrosive to steel. In natural gases the partial pressure of CO₂ is related to solubility in water. In buffered brines, pH is often in the range of 5 < pH < 7. The overall corrosion reaction is



Higher pH decreases the solubility of iron carbonate, leading to the growth of denser (more protective) scales on a steel surface¹⁸ and providing a diffusion barrier for the species that cause the corrosion. By adding a small amount of NaOH (or KOH), we eliminate foaming, maximize AA performance, and reduce corrosion in steel pipes. Since there are no notable differences in antiagglomeration for the same molar concentrations of NaOH and KOH (not shown for brevity), NaOH is preferred because of its lower molecular weight and cost.

We also investigate the effectiveness of AA at different cooling rates, a key factor for applications. In flowlines, the temperature drops slowly during transportation. However, the temperature decreases much faster in shut-in conditions and in the conditions for oil/gas capture in deepwater when the gas and/or oil mixes with cold seawater. We perform tests at cooling rates of -2 and -10 °C/h. At a fast cooling rate (-10 °C/h), we find that the 0.2 wt % AA is not effective because of a higher hydrate growth rate and higher hydrate nucleation. A higher AA concentration may be required in antiagglomeration. With increase of AA dosage, foaming becomes a serious issue even with increase of the NaOH concentration to 0.8 wt %. To solve the foaming problem, we introduce a small amount of an oil (*n*-octane) into our formulation to serve as a defoamer. AA is soluble in *n*-octane; as little as 0.2 vol % *n*-octane eliminates the foam formation completely. In the rocking process, we observe that small oil droplets are dispersed in the aqueous phase, which might promote the adsorption of AA molecules onto hydrate particle surface. The formulation with 0.3 wt % AA, 0.6 wt % NaOH, and 0.4 vol % *n*-octane successfully provides hydrate antiagglomeration of the natural gas at the initial pressure as high as 100 bar. Table 2 presents the concentration of *n*-octane and NaOH in our formulation in various tests. As the pressure increases, there is need for higher concentration of NaOH and higher concentration of *n*-octane. The higher concentration of NaOH relates to the need for increase of the pH with higher solubility of CO₂ in water. The higher concentration of *n*-octane relates to elimination of foaming and subsequent adsorption of AA at higher cooling rates. As Table 2 shows, 0.4 wt % NaOH and 0.2 wt % AA result in antiagglomeration at 80 bar when the cooling rate is slow (-2 °C/h), but the formulation becomes ineffective at high cooling rate (-10 °C/h). Adding 0.2 vol % *n*-octane solves this problem. Figure 5 presents the successful antiagglomera-

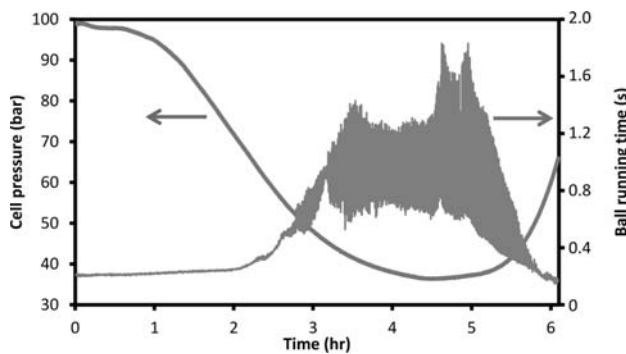


Figure 5. Natural gas: hydrate formation from the initial pressure of 100 bar and the initial temperature of 20 °C. The temperature decreases from 20 to 2 °C at a rate of -10 °C/h, then kept at 2 °C for 2 h before ramping back to 20 °C. The watercut is 99.6% (0.4 vol % *n*-octane). The concentration of AA is 0.4 wt %. NaOH concentration is 0.6 wt %.

tion of the natural gas hydrate from a pressure of 99 bar at a cooling rate of -10 °C/h, in which the formulation of 0.4 wt % AA, 0.6 wt % NaOH, and 0.4 vol % *n*-octane is used. Hydrate starts to form at 19.6 °C and 97.6 bar. The pressure decreases to 36.4 bar when the temperature is kept at 2 °C. When the ball running time is long, there are always fluctuations in data due to the slow ball movement. When the pressure goes below 50 bar, the ball running time becomes greater than 0.5 s, which is different from the data in Figure 4. In the test at 87 bar initial pressure in the natural gas, the pressure decrease is about 50 bar. From the initial pressure of 99 bar, the pressure decrease is about 62.6 bar, implying 25% more hydrate content in the mixture than the test at the initial pressure of 87 bar. Such high hydrate content increases the slurry viscosity.

As mentioned in ref 5, the cmc of our AA surfactant in water is 30 ± 3 ppm. The size of the micelles is measured by dynamic light scattering (DLS) to be 8.8 ± 1.3 nm. When the dosage is 2000 ppm (0.2 wt %), we observe a very thin layer of the surfactant rich phase at the top layer when the vial is allowed to stay still. After a 2 min handshaking, the surfactant molecules form aggregates with the average size of 1.0 ± 0.2 μm, measured by DSL within 30 s. Once 1.0 vol % *n*-octane is added, oil-in-water emulsions are formed with size of 54.6 ± 4.9 nm. In this case, most surfactant molecules can be evenly distributed in the aqueous phase, and there is no foam formation. Such distribution helps with a quick adsorption of AA molecules onto the hydrate particle surface. We believe this is the mechanism through which a small amount of *n*-octane strengthens the performance of our AA.

Higher AA dosage may also contribute to the kinetic inhibiting effect. As shown in Figure 6, hydrate starts to form at

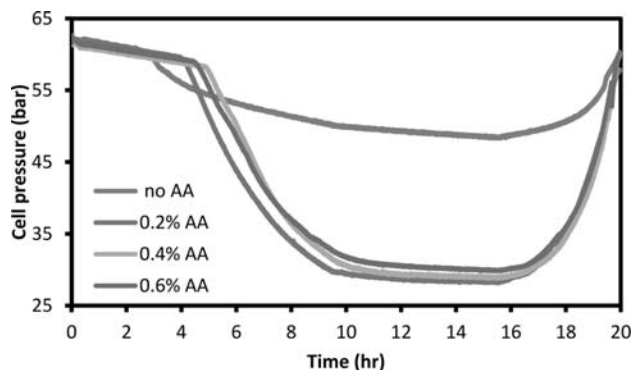


Figure 6. Natural gas: hydrate formation from the initial pressure of 62 bar at 20 °C. The temperature decreases from 20 to 2 °C at a rate of -2 °C/h, then kept at 2 °C for 2 h before ramping back to 20 °C. The watercut is 100%. The concentration of AA varies from 0 to 0.6 wt %. NaOH concentration is 0.4 wt %, and *n*-octane is 0.4 vol %.

16.0 °C and 60 bar without AA in the system. Without AA, hydrate solids limit the mass transfer from gas phase to liquid phase. The hydrate barrier blocks the transfer of gas to the rest of the aqueous phase; as a result, the hydrate formation rate becomes low, indicated by the slow pressure drop. Once the AA is added, hydrate formation is delayed. The hydrate formation temperature is 12.9 °C at 59.4 bar when AA concentration is 0.2 wt %. At 0.4 and 0.6 wt %, the hydrate formation temperatures are 11.8 (58.4 bar) and 12.2 °C (59 bar), respectively. The cell pressure at 2 °C is higher when the AA dosage is higher, indicating less hydrate content in the slurry.

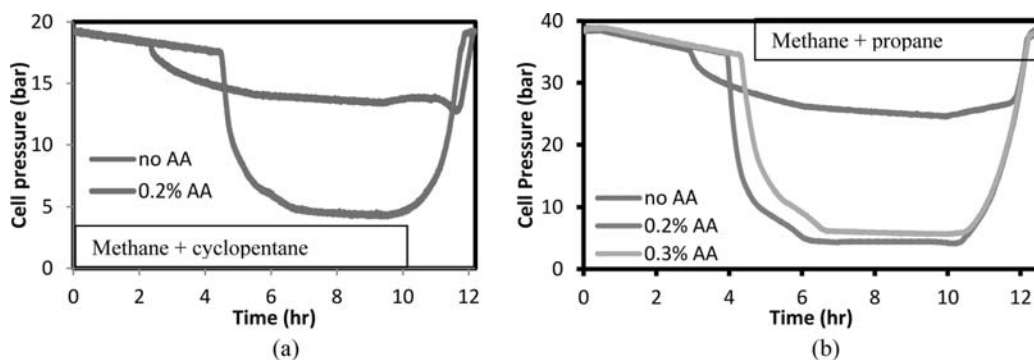


Figure 7. Hydrate formation pressure profiles of (a) methane + cyclopentane and (b) methane + propane systems. The temperature decreases from 20 to 2 °C at a rate of -4 °C/h, then kept at 4 °C for 4 h before ramping back to 20 °C.

In our work in methane hydrates, unlike the natural gas system, we did not observe a kinetic effect when AA was effective in antiagglomeration. The difference between methane and natural gas hydrates is in the hydrate structure. Methane forms sI, and natural gas forms sII hydrates. We have studied hydrate antiagglomeration in two other sII hydrates to establish the link between kinetic effects and hydrate structure. Figure 7a shows the hydrate formation temperature decrease in the methane + cyclopentane hydrates. The cell contains 1 mL of cyclopentane and 9 mL of H_2O in the initial mixture and is pressurized by methane. Without AA, hydrate forms at 15 °C (18.2 bar), and plugging occurs immediately. The plugging limits the mass transfer of gas phase to free water, thus slowing hydrate growth rate as mentioned above. By addition of 0.2 wt % AA, hydrate forms at 6 °C (17.7 bar), a 9 °C decrease. Figure 7b presents the hydrate formation temperature in the methane + propane system. The cell is charged with 1 mL of propane liquid (and 9 mL of H_2O) before charging methane to reach final pressure. The hydrate formation temperatures are 14.4 °C (36.0 bar), 10.3 °C (35.1 bar), and 9.2 °C (34.6 bar) at the AA concentrations of 0, 0.2, and 0.3 wt %, respectively. The results of natural gas, mixtures of methane and cyclopentane, and mixtures of methane and propane indicate a strong kinetic inhibiting effect in structure II (sII) hydrates. We do not observe appreciable kinetic effect in structure I (sI) hydrates.

All of the above results relate to DI water. We also perform a test in 1.5 wt % NaCl brine. The results are presented in Figure 8. The cells are cooled from 20 to 2 °C at a rate of -4 °C/h. Then they are kept at 2 °C for 2 h before being heated back to 20 °C. Without NaOH (blue), serious foaming is observed and the initial ball running time is high. Plugging occurs soon after hydrate starts to form at 17.6 °C and 67 bar. With 0.4 wt % NaOH, no foam is observed and antiagglomeration is observed. Hydrate starts to form at 12.0 °C and 65 bar, a strong kinetic effect. The ball running time is low throughout the test, indicating that the hydrate slurry has low viscosity as indicated in Figure 8.

CONCLUSIONS

We have demonstrated the effectiveness of a new formulation in hydrate antiagglomeration in a natural gas at low dosage at 100% watercut in both freshwater and brine, a hydrate slurry of low viscosity, kinetic inhibiting effect, and protection of steel pipeline. Our formulation contains a nonionic surfactant, a base to increase pH, and an oil to eliminate foaming. The three components show synergistic benefits to deliver a highly

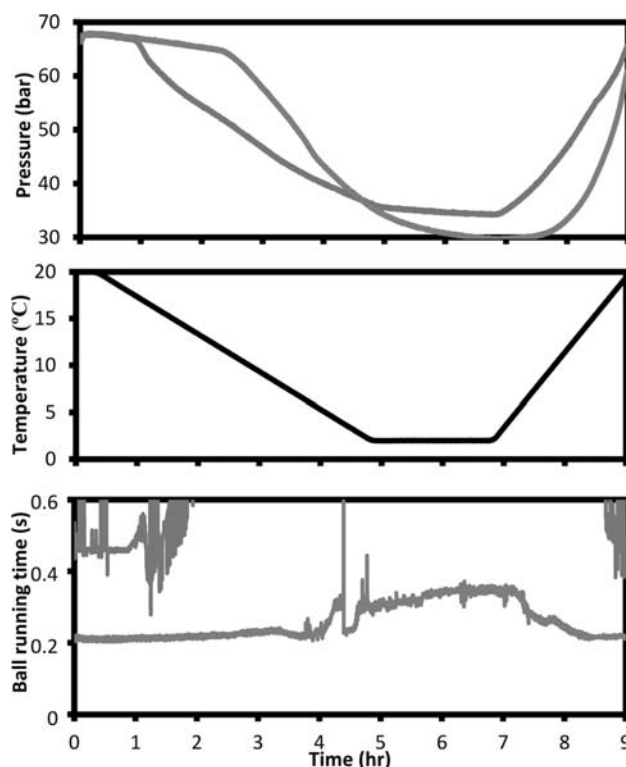


Figure 8. Natural gas: hydrate formation from the initial pressure of 68 bar at 20 °C. The temperature decreases from 20 to 2 °C at a rate of -4 °C/h, then kept at 2 °C for 2 h before ramping back to 20 °C. The watercut is 100%, and salinity is 1.5 wt % (NaCl brine). The concentration of AA is 0.2 wt %. NaOH concentration is 0.4 wt % (red) and 0 wt % (blue).

effective performance. This work extends our research from structure I hydrates to a much broader range of hydrate species.

The effectiveness of our AA at 100% watercut cannot be explained by the traditional water-in-oil emulsion theory.^{2,4,13,15–17} We have recently proposed a new mechanism based on the micelle formation and equilibrium among the adsorbed surfactants on the hydrate interface, the dispersed molecules, and the micelles in the aqueous phase.⁵ In this work we discuss complexities from an acid gas such as CO_2 in natural gases in hydrate antiagglomeration. We also discuss the relevant mechanisms and suggest the use of a small amount of a base and a small amount of an oil to achieve hydrate antiagglomeration. For a deeper understanding of the

processes, both hydrate particle size measurements and detailed molecular simulations are underway. Results will be published as those investigations become complete.

AUTHOR INFORMATION

Corresponding Author

*E-mail: abbas.firoozabadi@yale.edu.

Notes

The authors declare no competing financial interest.

ACKNOWLEDGMENTS

We thank the member companies of the Reservoir Engineering Research Institute (RERI) for their financial support.

REFERENCES

- (1) Koh, C. A.; Westacott, R. E.; Zhang, W.; Hirachand, K.; Creek, J. L.; Soper, A. K. Mechanisms of gas hydrate formation and inhibition. *Fluid Phase Equilib.* **2002**, *194*, 143–151.
- (2) Kelland, M. A. History of the development of low dosage hydrate inhibitors. *Energy Fuels* **2006**, *20* (3), 825–847.
- (3) Wu, M.; Wang, S.; Liu, H. A study on inhibitors for the prevention of hydrate formation in gas transmission pipeline. *J. Nat. Gas Chem.* **2007**, *16* (1), 81–85.
- (4) Huo, Z.; Freer, E.; Lamar, M.; Sannigrahi, B.; Knauss, D. M.; Sloan, E. D. Hydrate plug prevention by anti-agglomeration. *Chem. Eng. Sci.* **2001**, *56* (17), 4979–4991.
- (5) Sun, M.; Firoozabadi, A. New surfactant for hydrate anti-agglomeration in hydrocarbon flowlines and seabed oil capture. *J. Colloid Interface Sci.* **2013**, *402*, 312–319.
- (6) Klomp, U. C.; Kruka, V. C.; Reijnhart, R. WO Patent Application 95/17579, 1995.
- (7) Klomp, U. C.; Kruka, V. R.; Reijnhart, R.; Weisenborn, A. J. Method for inhibiting the plugging of conduits by gas hydrates. U.S. Patent 5648575, 1997.
- (8) Klomp, U. C.; Reijnhart, R. Method for inhibiting the plugging of conduits by gas hydrates. U.S. Patent 5879561, 1999.
- (9) Klomp, U. C. Method for inhibiting the plugging of conduits by gas hydrates. U.S. Patent 6152993, 2000.
- (10) Mokhatab, S.; Wilkens, R. J.; Leontaritis, K. J. A review of strategies for solving gas-hydrate problems in subsea pipelines. *Energy Sources, Part A* **2007**, *29* (1), 39–45.
- (11) Panchalingam, V.; Rudel, M. G.; Bodnar, S. H. Methods for inhibiting hydrate blockage in oil and gas pipelines using amide compounds. U.S. Patent 7381689, 2008.
- (12) Chua, P. C.; Kelland, M. A. Study of the gas hydrate anti-agglomerant performance of a series of *n*-alkyl-tri (*n*-butyl) ammonium bromides. *Energy Fuels* **2013**, *27* (3), 1285–1292.
- (13) Sloan, E. D.; Koh, C. A. *Clathrate Hydrates of Natural Gases*; CRC: Boca Raton, FL, 2008.
- (14) Turner, D. J.; Miller, K. T.; Sloan, E. D. Direct conversion of water droplets to methane hydrate in crude oil. *Chem. Eng. Sci.* **2009**, *64* (23), 5066–5072.
- (15) Mehta, A. P.; Hebert, P. B.; Cadena, E. R.; Weatherman, J. P. Fulfilling the promise of low-dosage hydrate inhibitors: journey from academic curiosity to successful field implementation. *Old Prod. Facil.* **2003**, *18* (1), 73–79.
- (16) Sloan, E. D. A changing hydrate paradigm—from apprehension to avoidance to risk management. *Fluid Phase Equilib.* **2005**, *228*, 67–74.
- (17) Zanota, M. L.; Dicharry, C.; Graciaa, A. Hydrate plug prevention by quaternary ammonium salts. *Energy Fuels* **2005**, *19* (2), 584–590.
- (18) DeWaard, C.; Williams, D. E. Prediction of carbonic acid corrosion in natural-gas pipelines. *Ind. Finish. Surf.* **1976**, *28* (340), 24–26.
- (19) Nestic, S. Key issues related to modelling of internal corrosion of oil and gas pipelines: a review. *Corros. Sci.* **2007**, *49* (12), 4308–4338.

(20) Colombel, E.; Gateau, P.; Barre, L.; Gruy, F.; Palermo, T. Discussion of agglomeration mechanisms between hydrate particles in water in oil emulsions. *Oil Gas Sci. Technol.* **2009**, *64* (5), 629–636.

(21) Nestic, S.; Nordsveen, M.; Nyborg, R.; Stangeland, A. A mechanistic model for carbon dioxide corrosion of mild steel in the presence of protective iron carbonate films—Part 2: A numerical experiment. *Corrosion* **2003**, *59* (6), 489–497.

(22) Nordsveen, M.; Nestic, S.; Nyborg, R.; Stangeland, A. A mechanistic model for carbon dioxide corrosion of mild steel in the presence of protective iron carbonate films—Part 1: Theory and verification. *Corrosion* **2003**, *59* (5), 443–456.